Prepublished Copy

NATURE ENVIRONMENT AND POLLUTION TECHNOLOGY

Article In Press

PEER-REVIEWED PREPUBLISHED MANUSCRIPT

This is a peer-reviewed prepublished version of the paper to be published in **Vol. 26, No. 1, March 2027.**

Paper Mill Sludge Derived Biochar and Magnetic Biochar for simultaneous removal of COD and TDS from dye wastewater

Charmiben Panchani, Vishwa Vraj Shah and Ahaan Thakore

RECEIVED
26 March 2026

CITE THIS ARTICLE
Panchani, C., Shah, V.V. and Thakore, A., 2027. Paper Mill Sludge Derived Biochar and Magnetic Biochar for simultaneous removal of COD and TDS from dye wastewater. Nature Environment and Pollution Technology, 26(1), B4442.

https://doi.org/10.46488/NEPT.2027.v26i01.B4442

EARLY-ACCESS STATEMENT

This manuscript, after peer review, is being released online in its original, unedited form to provide early access to its findings. Prior to final publication, it will undergo additional editing and formatting. Readers may note that, as an unedited version, the manuscript may have linguistic and other minor errors. The DOI will be active after the final publication of the paper.

PUBLICATION STATUS

PEER REVIEW	ONLINE VERSION	FINAL ISSUE
Completed	**Prepublished**	**March 2027**

Original Research Paper

Paper Mill Sludge Derived Biochar and Magnetic Biochar for simultaneous removal of COD and TDS from dye wastewater

Charmiben Panchani, Vishwa Vraj Shah, Ahaan Thakore†

Department of Environmental Engineering, L.D. College of Engineering, Ahmedabad, 380015, Gujarat, India

† Corresponding Author: Ahaan Thakore; Email: ahaanthakore@gmail.com

ORCID IDs: [1]0009-0009-3927-4213, [2]0000-0002-6192-0084, [3]0009-0008-7059-0495

,

Abstract: Dye wastewater, characterized by high chemical oxygen demand (COD) and total dissolved solids (TDS), poses significant environmental challenges. This study addresses the limited evidence on the use of paper mill sludge (PMS) as biochar for simultaneous COD and TDS removal in real-world effluent. PMS was converted to magnetic biochar via slow pyrolysis at 500 °C. Adsorbents were characterized using proximate analysis, iodine number, SEM, BET and FTIR. Batch adsorption experiments evaluated the effects of pH, adsorbent dosage, and contact time. Results indicated that magnetic biochar outperformed biochar. Under optimized conditions (pH 3, dosage 2.0 g/50 mL, contact time 180 min), biochar achieved COD and TDS removal efficiencies of 78 ± 1.2% and 71 +1.1%. In contrast, magnetic biochar achieved 86 ± 1.4% COD and 91 ± 1.2% TDS removal. Superior performance is attributed to modifications in surface characteristics and increased active adsorption sites. Overall, this study demonstrates the effective, sustainable application of PMS-derived biochar and magnetic biochar for the simultaneous removal of COD and TDS from real dye wastewater, providing a viable pathway for the valorization of industrial waste.

Keywords: Chemical oxygen demand (COD), Dye wastewater, Paper mill sludge Biochar (PBC), Paper mill sludge magnetic Biochar (PMBC), Slow pyrolysis

1. INTRODUCTION

Paper Mill sludge is a byproduct generated from the clarification of liquid waste in pulp and paper mills. They are generated in large quantities, thereby creating major disposal challenges. Sludge is primarily composed of organic materials such as lignin, cellulose, and hemicellulose (Turner et al., 2022), with varying ash content depending on the industrial operations. Untreated sludge can lead to high BOD and COD concentrations (Dhinesh et al., 2024) if discharged into water bodies, posing a clear threat to aquatic life. Currently, incineration is used to dispose of paper mill sludge; however, this method emits particulate matter and sulfur dioxide into the air, and, if landfilled, it contaminates soil by introducing heavy metals. Because the sludge generated is in a semi-solid state and in slurry

form with 30% moisture content of the total mass. Considering its environmental impact, the reusability of paper mills is a good alternative for biochar production (A G et al., 2026). Paper mill sludge is a good candidate for soil conditioning, fertilization, material recovery, and as an adsorbent for pollution control. Hence, sludge was selected as a viable precursor for biochar production, fulfilling the goal of reusability and contributing to the circular economy. The biochar formed can be highly effective owing to the rich organic content of paper mill sludge.

Biochar (BC) is a carbon-rich material produced by thermal conversion in an oxygen-controlled environment. Raw materials used for the preparation of biochar (BC) can be derived from plant, animal, or sludge-based sources(Simões dos Reis et al., 2022). Plant-based sources used for the manufacturing of adsorbents include agricultural waste and forest waste. Likewise, cattle, chicken, shell bones and nutmeg shells(Ishar et al., 2024) are used as raw materials for the production of adsorbents. Sludge-based raw materials are industrial sludges from various industries, are rich in carbonaceous material, and can be synthesized via slow, fast, and flash pyrolysis. In the context of the three processes above, slow pyrolysis can produce more char. It is a thermal conversion process characterized by long residence times and slow heating rates, resulting in almost equal amounts of solid and gaseous products. In this process, different types of reactors can be used for biochar production, with heat provided by partial combustion of the feed, external heaters, or hot gas recirculation. These conditions enhance the biochar yield by increasing cracking reactions that reduce the production of liquids or bio-oils. Comparative analysis suggests that biomass with high lignin and ash contents, along with large particle size, enhances biochar output under slow pyrolysis conditions.

Biochar, with its characteristics of high surface area, volatility, high carbon and ash content, favourable pore size (Igalavithana et al., 2020), and low alkaline pH, is suitable for use as an adsorbent medium.(Devi and Saroha, n.d.). Biochar has strong adsorptive properties, but its recovery remains a significant challenge. This leads to the wastage of valuable resources and can result in secondary pollution. Magnetic biochar can provide an edge over conventional biochar owing to its magnetic properties, which enable straightforward physical separation from treated effluent using an external magnet—a significant practical advantage over conventional biochar, which requires filtration. Whether the recovered material can be regenerated and reused depends on the desorption characteristics, which were not investigated in this study. A critical limitation of biochar (BC) is that it cannot be separated from the secondary medium, which hinders the goal of ecological balance. To overcome this limitation, metal salts or their oxides can be synthesized. Biochar (BC) can be modified with various alkalis or metal oxides, thereby significantly enhancing the adsorbent's surface area and adsorption capacity for pollutant removal ;(Fakhar et al., 2025) (Habila et al., 2023) A transition metal or its oxide was incorporated into the given product to form Magnetic Biochar (MBC) (Zhao et al., 2021), which can be recovered more easily than the original product. The methods used to prepare magnetic biochar (MBC) are listed in **Table 1.**

Table 1: Methods for the Preparation of Magnetic Biochar (MBC)

Type of Method	Description
Impregnation Pyrolysis	Biochar impregnation in solution containing transition metals and consequently removal of solvent after pyrolyzing the dried residue in muffle furnace with limited oxygen supply.
Co – precipitation	Dispersion of biochar in transition metal solution with addition of metal compounds to achieve pH 9-11. Supernatant is removed and dried, after which MBC is collected using magnet.
Reductive – deposition	Use of reducing agents for transition metals in solvent medium. After which supernatant is dried and MBC is collected
Hydrothermal – carbonization	Heterogenous reaction of raw material with metal ion solution at low temperature (100 - 200°C) followed by pyrolysis.

According to the Annual Survey of Industries 2022-23, Gujarat has 29,766 manufacturing factories, among which approximately 1,500 dye and dye intermediate manufacturing units, according to the Gujarat Dyestuff Manufacturers Association (GDMA). Effluent generated by the dye industry is considered harmful due to its contaminating properties (Islam et al., 2025). These include colour, total dissolved solids (TDS), total suspended solids (TSS), biochemical oxygen demand (BOD), chemical oxygen demand (COD) and heavy metal concentration (Wang et al., 2022). Generally, methods for treating dye effluents can be classified into physical and chemical treatments, which include oxidation, ozonation, electrolysis, adsorption, and filtration (Al-Tohamy et al., 2022). Among these methods, oxidation and ozonation have high operational costs due to the need for precise reaction conditions and the generation of ozone, which must be on-site because of its short half-life. Electrolysis has a high energy demand and requires special electrodes and equipment. At the same time, the filtration method can remove dissolved dyes to a certain extent but is often prone to membrane fouling and clogging (Tanveer et al., 2023) In contrast, adsorption has a higher removal rate for a wide range of dyes, is easy to operate and scale, and is cost-effective. Therefore, adsorption is a viable treatment method (Kathing and Saini, 2022). Adsorption can adopt various mechanisms for pollutant removal, such as pore filling, Hydrophobic partitioning, electrostatic interactions, and electron donor-acceptor (EDA) interactions (Lima et al., 2019). Activated charcoal generally adopts a pore-filling adsorption mechanism owing to its high porosity. Conventionally, industries use Activated Carbon as an adsorbent (Husien et al., 2022), but the major drawback of this material is its high cost. Therefore, economical and eco–friendly alternatives are required for large-scale deployment (Nizam et al., 2021)

In the present study, paper mill sludge-derived biochar (PBC) and magnetic biochar (PMBC) were used to treat real dye effluent from an industry in Gujarat, which has high COD and BOD values and is not deemed safe for untreated discharge. This study demonstrates the use of paper mill sludge, an abundant yet problematic industrial waste, as a valuable adsorbent. It offers a view of the use of the adsorbent for the treatment of actual effluent from dye industries, characterized by high COD and TDS values, which can make the wastewater highly non-biodegradable. The generated sludge is rich in cellulose, hemicellulose, and lignin, which are similar in characteristics to those of wood from trees. Therefore, this adsorbent can be used instead of virgin resources. This study extends beyond conventional biochar (PBC) by producing magnetic biochar (PMBC) from paper mill sludge (Santhosh et al., 2020) using a co-precipitation method that can be easily adopted (Guel-Nájar et al., 2023). Several studies have explored

the use of PMS as a raw material for biochar preparation, mainly focusing on soil amendment or CO_2 sequestration methods(Devi and Saroha, 2014a; Igalavithana et al., 2020). To the best of our knowledge, no previous study has (i) synthesised magnetic biochar specifically from paper mill sludge via co-precipitation, (ii) utilised the produced material for COD and TDS removal, (iii) tested it with actual industrial effluents instead of synthetic dye wastewater. Hence, this study serves dual purposes: utilising industrial waste as a resource for real effluent treatment and addressing the problem of biochar recovery from aqueous solutions, as shown in **Figure 1**.

Figure 1: Conceptual diagram of Paper Mill Sludge Derived Biochar (PBC) and Magnetic biochar (PMBC) for Dye Wastewater Treatment

Hence, this study offers a simple solution for efficient recovery and reusability after the adsorption process through magnetic separation. This novel approach offers an economical material for wastewater treatment that can be

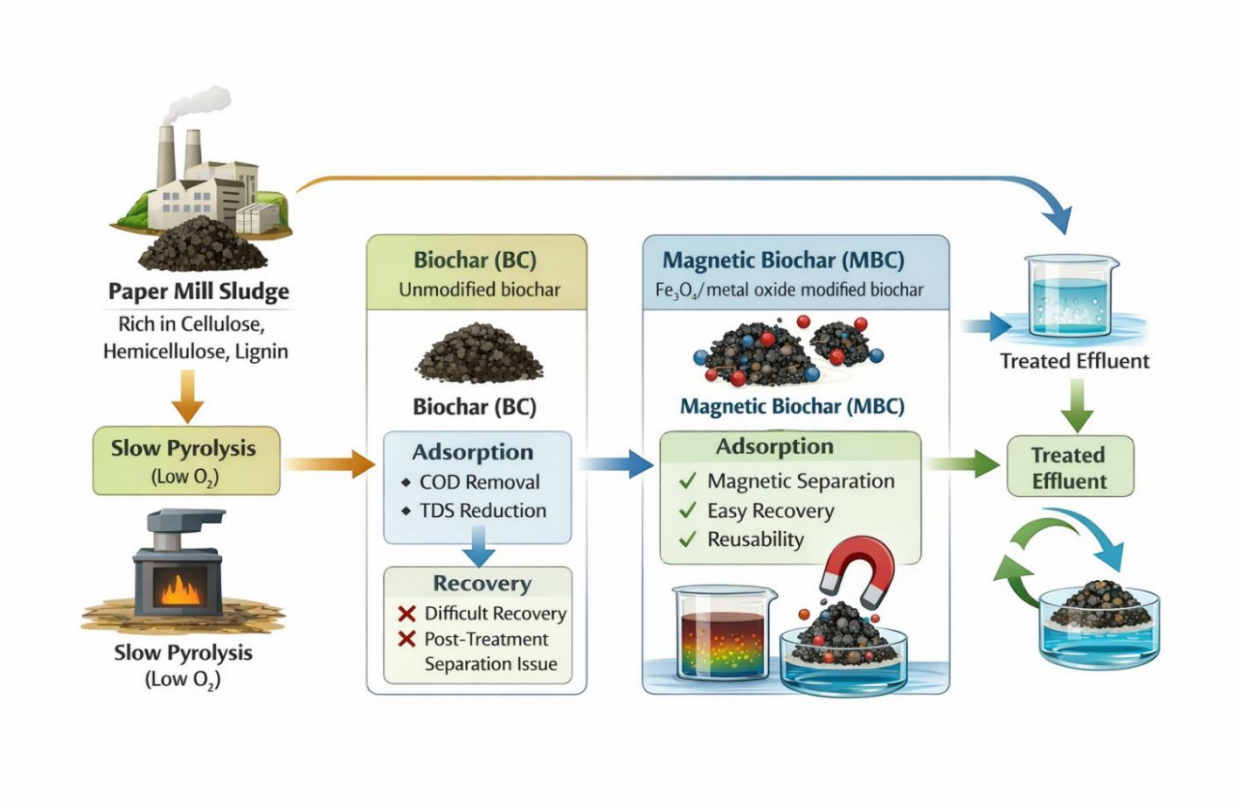

magnetically recovered post-treatment, with reusability potential pending further regeneration studies.

2. MATERIALS AND METHODS

2.1 Biochar and Magnetic Biochar Synthesis

Processed Paper mill sludge is collected from one of the industries situated at Ankleshwar, Gujarat.

The sludge obtained has approximately 30% moisture content, so pre-treatment is necessary in order to remove the moisture. It includes a 2-step process: drying the sludge in the sun for 2 days. The second step was to further dry the sludge in a hot-air oven at 105℃ for 12 h. Biochar was produced at the lab scale in a muffle furnace. The processed paper mill sludge, which is rich in lignin, undergoes dissociation at 450 – 500 ℃. The sludge was placed in a crucible and pyrolyzed in a muffle furnace at 500 ℃ for 2 hours at a heating rate of 10 ℃/min (Devi and Saroha, 2014a). After the given time period, the product thus formed was cooled and crushed into a powder < 75µm. The temperature maintained during pyrolysis is an influential factor in determining biochar characteristics. At higher temperatures, the micropore volume increased substantially owing to the dissociation of cellulose and hemicellulose (Simões dos Reis et al., 2022). This breakdown of the complex compound creates a void between the particles, increasing the total surface area of the adsorbent material.

For the synthesis of magnetic biochar (PMBC), a co-precipitation method was adopted by adding iron composites of $FeSO_4.7H_2O$ and $FeCl_3.6H_2O$ in proportions of 1:1 and 1:2, respectively, as shown in **Figure 2.** The preparation was performed using 3.66 grams $FeSO_4 \cdot 7H_2O$ and 6.66 grams $FeCl_3 \cdot 6H2O$ at a composite ratio of 1:2. The two components were dispersed in 200 mL of distilled water in a beaker and stirred continuously for 1 h to oxidize Fe^{2+} to Fe^{3+}. The pH range was adjusted to 10-11 by adding 1N Sodium Hydroxide solution (Lv et al., 2020). This process was followed by the addition of 10 grams of biochar. The suspension was stirred continuously for 1 h until Fe_3O_4 precipitates formed on the biochar surface under alkaline conditions. The stirred suspension was left overnight to achieve uniform settling, after which it was dried in a hot-air oven at 105℃ for 12 h.

Figure 2: Preparation of Magnetic Biochar

2.2 Characterization of Biochar and Magnetic biochar

2.2.1 Physicochemical characteristics

The physicochemical properties of biochar (PBC) and magnetic biochar (PMBC) were analyzed to evaluate their suitability as adsorbents for dye wastewater treatment. The adsorption efficiency is strongly influenced by the particle size, surface area, and surface chemistry, as smaller particle size and higher surface area provide a greater number of active adsorption sites. Proximate analysis of PBC and PMBC was carried out to determine the moisture

content, volatile matter, ash content, and fixed carbon, following IS 1350 (Part I): 1984 (Reaffirmed 2013). Moisture content reduces effective adsorption by occupying active sites, whereas volatile matter contributes to pore formation during pyrolysis. The ash content affects the surface properties and adsorption performance, whereas a higher fixed carbon content enhances adsorption owing to the improved surface area and structural stability.

2.2.2 Biochar Yield

The pyrolysis temperature, heating rate, and residence time primarily governed the biochar yield. Increasing the pyrolysis temperature resulted in enhanced devolatilization, thereby reducing the solid char yield. Previous studies have reported a decreasing trend in biochar yield with increasing temperatures (Devi and Saroha, 2014b). In the present study, paper mill sludge was subjected to slow pyrolysis at 300 °C and 500 °C in a muffle furnace under limited oxygen conditions. The biochar yield was calculated using **Eq. No. 1**

$$\text{Biochar yield} = \frac{\text{Mass of biochar}}{\text{Mass of dry sample}} * 100 \quad \text{----------} \quad (1)$$

2.2.3 Iodine Number

The iodine number is an important parameter for evaluating the microporous structure and surface area of carbonaceous adsorbents. It is expressed as milligrams of iodine adsorbed per gram of material (mg g^{-1}). It represents the adsorption capacity for small molecular species and is widely used to assess the adsorption capacity of activated carbon and biochar. The iodine number of PBC and PMBC was determined according to ASTM D4607, which defines the iodine adsorption capacity as the amount of iodine adsorbed by 1 g of adsorbent when the residual iodine concentration in the filtrate is 0.02 N. For PMBC, iodine number was evaluated for samples prepared using $FeSO_4 \cdot 7H_2O$ and $FeCl_3 \cdot 6H_2O$ in molar ratios of 1:1 and 1:2, to assess the influence of iron loading on surface characteristics.

2.2.4 Morphological and Functional group analysis

The surface morphology and pore structure of PBC and PMBC were examined using scanning electron microscopy (SEM) to assess porosity, surface roughness, and structural heterogeneity. For PMBC, SEM analysis was used to confirm the successful impregnation and distribution of iron oxide nanoparticles on the biochar surface.

Functional groups present in PBC and PMBC were identified using Fourier transform infrared spectroscopy (FTIR). FTIR spectra revealed oxygen-containing functional groups, such as hydroxyl, carboxyl, and aromatic moieties, which play a crucial role in adsorption via electrostatic interactions, hydrogen bonding, and π–π interactions.

2.2.5 Magnetic Properties of Magnetic Biochar

The magnetic properties of PMBC were evaluated to determine its separation and recovery potential after adsorption. The bulk sigma magnetization was measured to assess the maximum magnetization achievable under an external magnetic field, which directly influences the magnetic separation efficiency(Muzenda and Arotiba, 2022). Iron oxide impregnation was carried out using $FeSO_4 \cdot 7H_2O$ and $FeCl_3 \cdot 6H_2O$ in molar ratios of 1:1 and 1:2, respectively, to enhance saturation magnetization while maintaining the adsorption performance. (Oliveira et al., 2002)

2.2.6 BET Surface Area and Pore Structure Analysis

The surface properties of PBC and PMBC were determined by N_2 adsorption–desorption (Ashapura Minechem Ltd.) Surface area (S_{BET}) was calculated using the Brunauer–Emmett–Teller (BET) methodology. Pore volume and pore size distribution were derived using the Barrett–Joyner–Halenda (BJH) method applied to the desorption isotherm.

2.3 Characterization of Dye effluent

The dye wastewater used in this present study was collected from a dye manufacturing unit located in Gujarat, India, and characterized prior to treatment. The physicochemical parameters analyzed included pH, chemical oxygen demand (COD), biochemical oxygen demand (BOD), total dissolved solids (TDS), and total suspended solids (TSS). The pH of wastewater was measured using a calibrated digital pH meter. COD and BOD were determined according to standard methods for the examination of water and wastewater, whereas TDS and TSS were measured gravimetrically. The BOD: COD ratio was calculated to assess the wastewater's biodegradability. The measured values were compared to the permissible discharge limits, and the results are presented in **Table 2**. Based on the initial characterization, biochar (PBC) and magnetic biochar (PMBC) were selected as adsorbents for the reduction of COD and TDS in dye wastewater. A BOD: COD ratio of 0.2 indicates that the wastewater is highly non-biodegradable (Al-Tameemi et al., 2022)

Table 2: Physicochemical Characterization of dye effluent and comparison with Permissible Limits

Parameter	Result	Permissible Limit
pH	6.5	7.5
COD	1354 mg/L	250 mg/L
BOD	300 mg/L	30 mg/L
TDS	5500 mg/L	2100 mg/L
TSS	108 mg/L	100 mg/L
BOD: COD Ratio	0.2	--

2.4 Batch Scale study

Optimization of pH, contact time, and adsorbent dosage for biochar (PBC) and magnetic biochar (PMBC) was conducted to evaluate their performance in reducing chemical oxygen demand (COD) and total dissolved solids (TDS) from dye wastewater. Batch adsorption studies were performed using 50 mL of primary treated dye effluent in 200 mL glass beakers, with varying adsorbent dosages under controlled pH and contact time conditions. The adsorption systems were agitated by magnetic stirring, followed by a settling period equivalent to half of the applied contact time, as shown in **Figure 3**. PBC was separated by filtration using Whatman No. 42 filter paper, whereas PMBC was recovered using an external magnetic field. The treated effluents obtained under different experimental conditions were analyzed for COD and TDS. All batch adsorption experiments were conducted in duplicate (n = 2), and the results are reported as mean ± standard deviation (SD). The coefficient of variation (CV) was maintained below 5% for all reported values, confirming experimental repeatability. Statistical comparisons of

PBC and PMBC removal efficiencies at optimal conditions were performed using an independent-samples t-test ($p < 0.05$).

The adsorption capacity (q, mg/g) was calculated using Equation 2:

$$q = (C_0 - C_e) \times V / m \quad \text{---------- (2)}$$

where C_0 (mg/L) and C_e (mg/L) are the initial and equilibrium concentrations of COD or TDS, respectively, V is the volume of solution (L), and m is the mass of adsorbent (g).

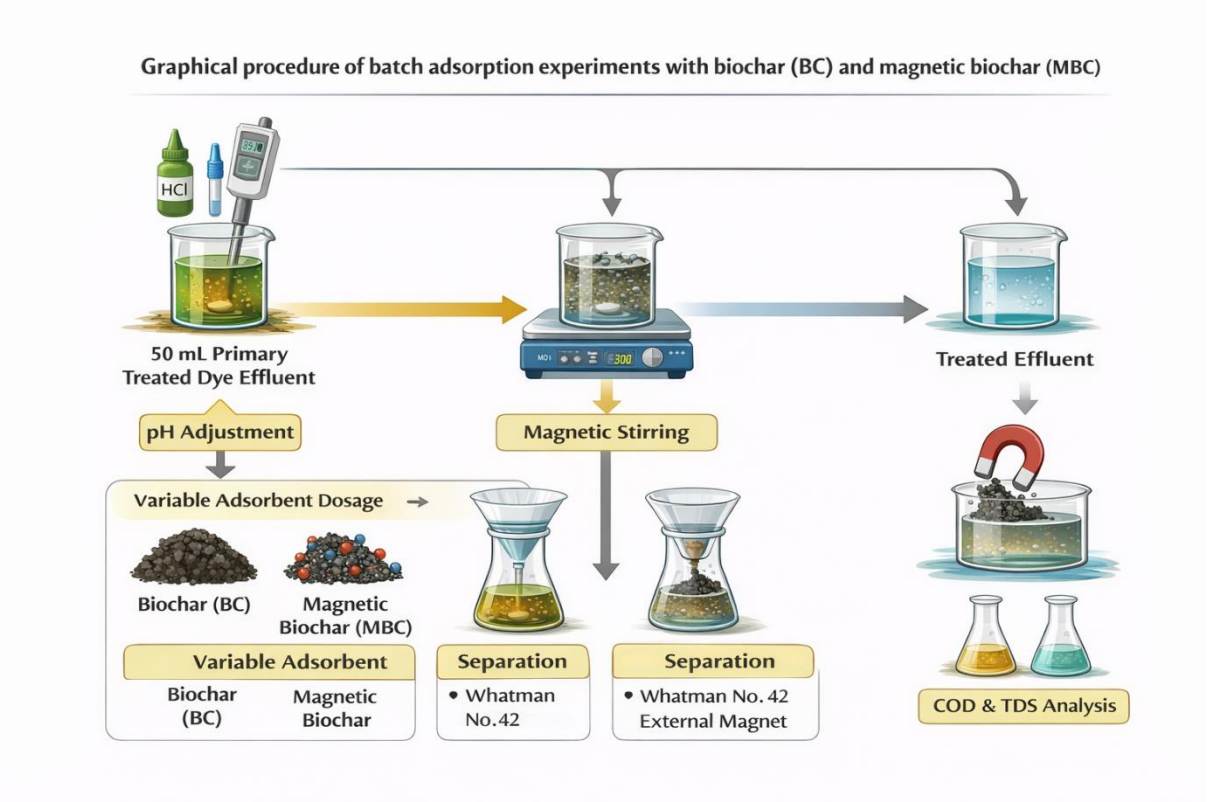

Figure 3: Batch adsorption study with PBC and PMBC for real dye wastewater

3. RESULTS AND DISCUSSION

3.1 Characterization of prepared biochar and magnetic biochar

Characterization of biochar results in a low moisture content of 2.90%, which increases the number of adsorption sites. The high volatile matter of 33.00% can enhance pore formation in the adsorbent (Leng et al., 2019), while the ash content of 42.60% influences the material's performance. The high fixed carbon of 21.50% can lead to robust adsorption owing to its surface area (Weber and Quicker, 2018). The results of proximate analysis are presented in **Table 3.**

Table 3: Proximate analysis of prepared Biochar and Magnetic Biochar

Sr. No.	Parameters	Biochar	Magnetic Biochar
		Results (%)	Results (%)
1	Moisture Content	2.90	1.90
2	Volatile Matter	33.00	22.50
3	Ash	42.60	52.15
4	Fixed Carbon	21.50	23.45

Moreover, Composite characterization was carried out for MBC, which determines a higher bulk sigma magnetization of 21 J/T/kg for the composite ratio of 1:1 for iron oxide, in which the Fe_2O_3 by mass was 66%, while for a composite ratio of 1:2, the Fe2O3 percentage concentration was comparatively low; hence, the bulk sigma magnetization was 9 J/T/kg (Zhang et al., 2021).

The second important parameter for the prepared biochar was biochar yield, which was influenced by pyrolysis temperature and heating rate. Pyrolysis temperature is the key factor influencing biochar yield, and as the pyrolysis temperature increases from 400°C to 1000°C, the yield decreases with respect to pyrolysis time and heating rate. Here, the maximum yield was observed at a low pyrolysis temperature of 300°C, with a 50% output, compared to 36% at 500°C (Amini et al., 2019) (Kan et al., 2016). The biochar yields of PBC and PMBC are listed in **Table 4.**

Table 4: Biochar yield at varying temperature and residence time

Temperature	Carbonization Time (minutes)	Heating Rate	Yield (%)
300°C	60	10°C/minute	50
500°C	120	10°C/minute	36

Moreover, the iodine number (IN) of PBC was 318 mg/g at a residence time of 1 h at 300°C. The iodine number was observed to double to 666 mg/g at 500°C and a residence time of just 20 min. For PMBC, the iodine number at the 1:1 Fe^{2+}: Fe^{3+} composite ratio was 327 mg/g, compared with 541 mg/g at the 1:2 ratio. The higher iodine number at 1:2 indicates lower total iron loading relative to biochar mass, leaving more micropore volume accessible for iodine uptake. Conversely, the 1:1 ratio deposited a greater iron oxide mass — as evidenced by its higher bulk sigma magnetisation (21 J/T/kg vs 9 J/T/kg) — which partially blocked micropores and reduced the iodine-accessible surface area. For adsorption experiments, the 1:2 ratio was selected because it strikes a better balance between surface area retention and magnetic functionality. This suggests the presence of magnetic biochar with a higher $FeCl_3$ mass concentration (Sayğılı and Güzel, 2016).

The prepared biochar and magnetic biochar were analyzed using advanced characterization techniques, including SEM and FTIR. The SEM micrograph of the biochar at 1000× magnification

reveals a highly irregular, rough, and heterogeneous surface structure, as shown in **Figure 4(a) and Figure 4(b).** The surface consisted of fragmented plate-like and flaky particles, with numerous voids, crevices, and inter-particle pores distributed throughout the matrix. Such morphological features are typically associated with the release of volatile components during pyrolysis, resulting in the formation of a porous carbonaceous framework.

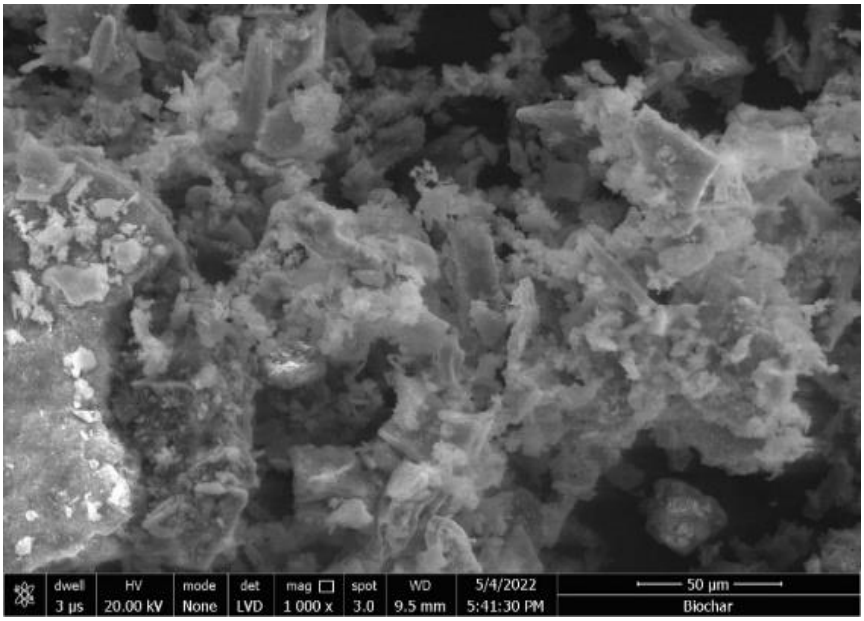

Figure 4(a): SEM image of the prepared biochar (PBC) from paper mill sludge at 500 °C (Low magnification)

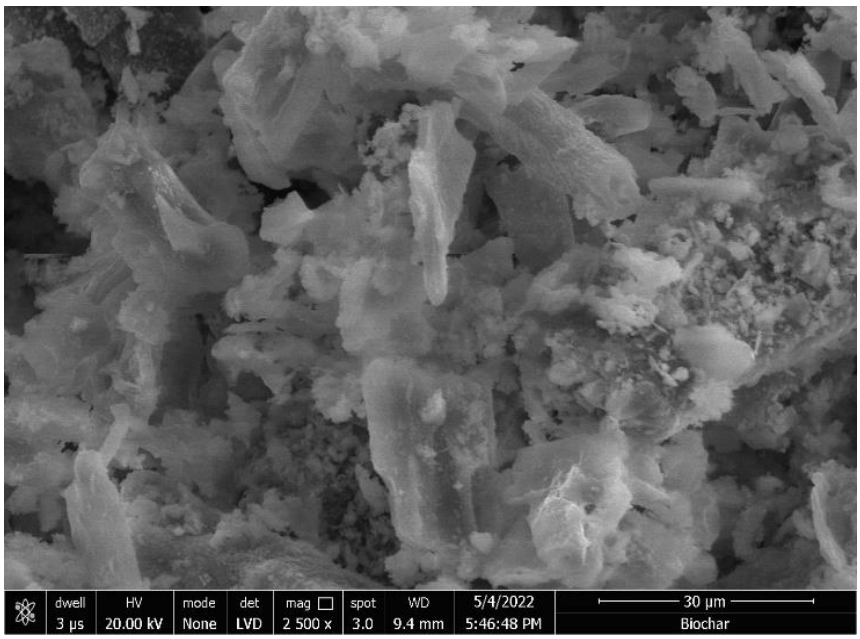

Figure 4(b): SEM image of the prepared biochar (PBC) from paper mill sludge at 500 °C (High magnification)

In comparison, the SEM images of the magnetic biochar in Figure 5(a) and Figure 5(b) show a denser, more compact morphology, with the surface partially covered by fine, granular, and clustered particles. These particles were attributed to the successful incorporation of magnetic iron-based phases onto the biochar surface. The magnetic particles appear to be non-uniformly distributed, forming localized agglomerates that adhere firmly to the biochar matrix.

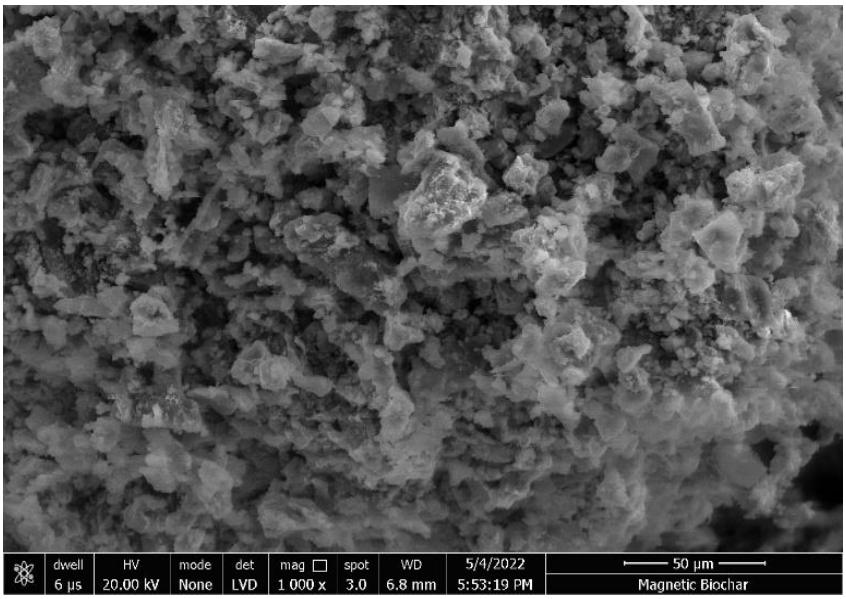

Figure 5(a): SEM image of the prepared magnetic biochar (PMBC) from paper mill sludge at 500 °C (Low magnification)

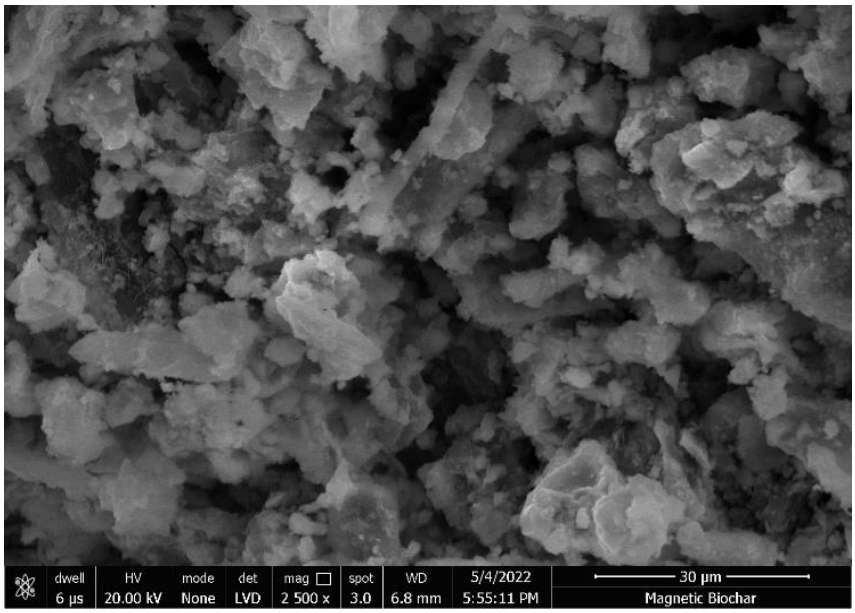

Figure 5(b): SEM image of the prepared magnetic biochar (PMBC) from paper mill sludge at 500 °C (High magnification)

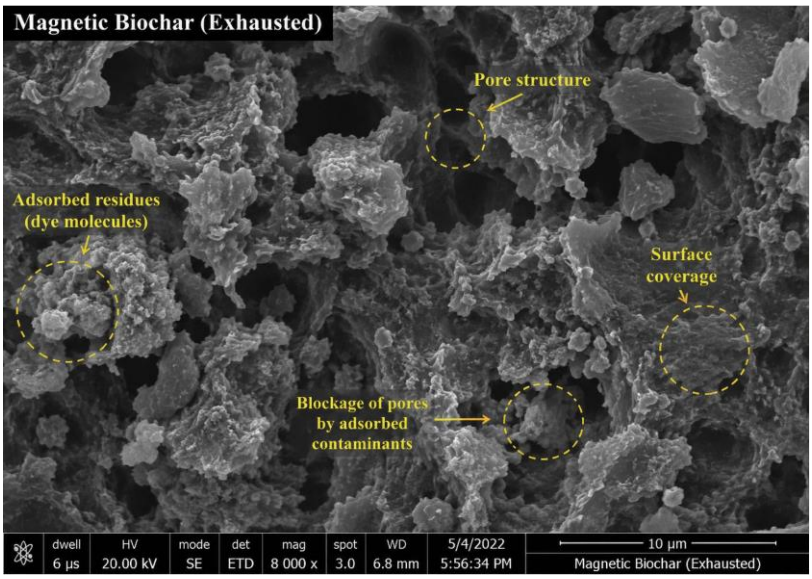

Figure 6: SEM image of the exhausted magnetic biochar (PMBC) from paper mill sludge at 500 °C (High magnification)

Figure 6 shows the SEM image of PMBC post adsorption. The well – defined pore structures and deep cavities appear significantly filled with adsorbed species. The surface exhibits a more congested structure compared to Fig. 5(a) and 5(b), which is attributed to the successful accumulation of dye molecules within the microporous and mesoporous framework. The clearly visible morphological changes corroborate the significant reductions observed

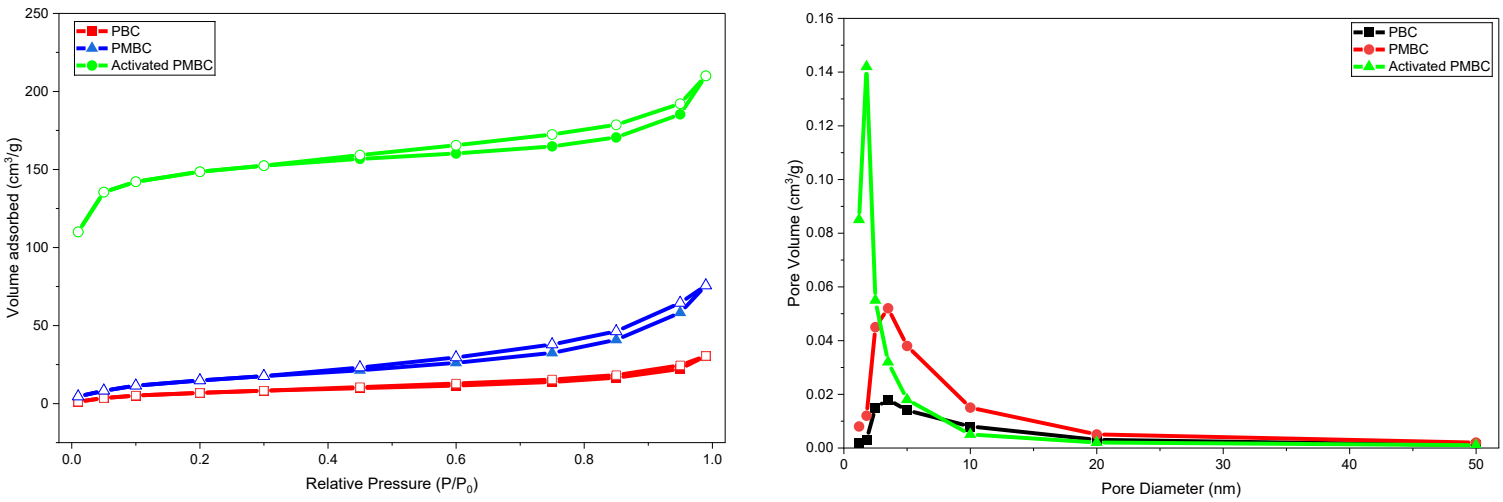

in COD and TDS during the batch studies.

Figure 7: N_2 adsorption–desorption isotherm and pore size distribution of PBC, PMBC and activated PMBC

PBC and PMBC exhibited low N_2 uptake, which is consistent with their BET surface areas of 40-50 m^2/g and 80-150 m^2/g, respectively. In contrast, activated PMBC, which is used in batch adsorption study, followed a Type I isotherm, depicting a highly microporous structure, supporting high surface area of >600m^2/g. BJH pore

distribution confirms a dominant pore volume concentration in the activated sample. Previous studies have reported paper mill sludge biochar in range of 43-80 m^2/g and chemical activation has resulted in surface areas of 430-600 m^2/g(Niu et al., 2025). (Liang et al., 2020)reported surface area of around 82 m^2/g of magnetically modified bagasse biochar. (Chistie et al., 2025)has shown a high surface area range of 265 – 385 m^2/g through acid activation and Fe_3O_4 modification in biochar made from areca husk. This study has critically shown that S_{BET} of PBC (48.2 m^2/g) aligns with the previous studies while PMBC has a higher pore size distribution and high S_{BET} characteristics of 642.8 m^2/g.

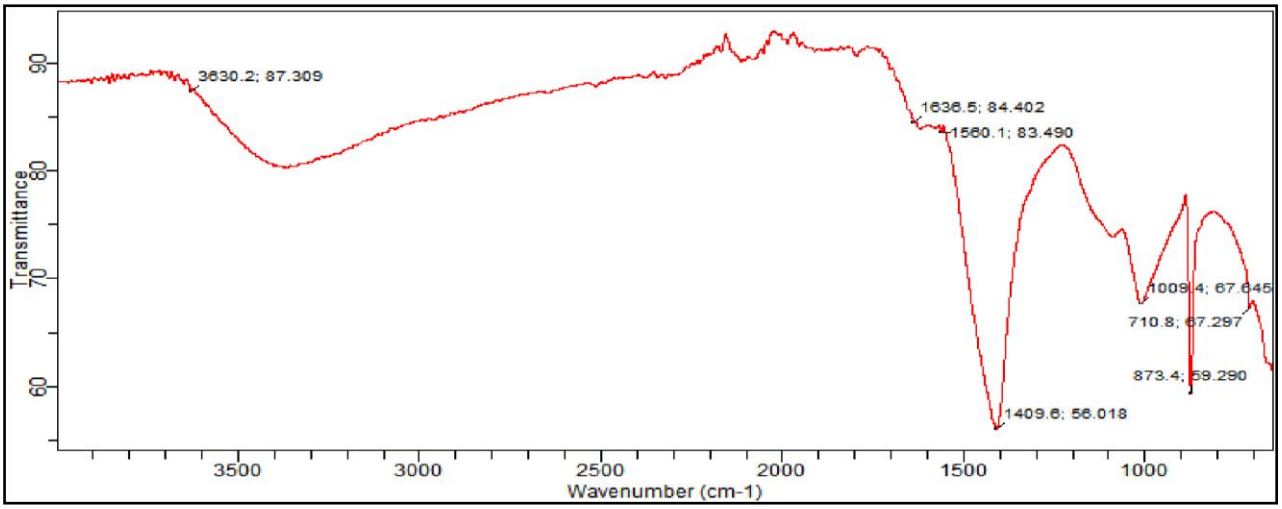

Figure 8: FTIR of the prepared magnetic biochar (PMBC)

The FTIR spectrum recorded in the range of 400–4000 cm^{-1} shows several characteristic absorption bands corresponding to oxygen-containing and aromatic functional groups on the biochar surface, as shown in **Figure 8**. A broad absorption band observed around 3630 cm^{-1} is attributed to the O–H stretching vibration of hydroxyl groups associated with phenolic, alcoholic, and adsorbed water molecules. The presence of hydroxyl groups indicates the biochar surface's hydrophilic nature and provides potential adsorption sites via hydrogen bonding and electrostatic interactions. The absorption peak appearing near 1638 cm^{-1} is assigned to C=O stretching vibrations of carbonyl or quinone groups and/or C=C stretching of aromatic rings, which are typically formed during the pyrolysis of lignocellulosic biomass. These functional groups contribute to surface polarity and enhance interaction with organic contaminants. The distinct band around 1580 cm^{-1} corresponds to aromatic C=C skeletal vibrations, confirming the formation of an aromatic carbon structure during thermal decomposition. This aromatic framework contributes to biochar's structural stability and supports adsorption via π–π interactions, particularly for aromatic dye molecules and organic pollutants. The strong absorption peak observed at 1409 cm^{-1} is attributed to C–H bending vibrations and/or O–H bending of carboxylate groups, suggesting the presence of surface carboxylic functionalities. These groups are known to play a significant role in adsorption via surface complexation and ion-exchange mechanisms, particularly at alkaline pH. The peak near 1009 cm^{-1} corresponds to the C–O stretching

vibrations of alcohols, phenols, or ether groups, indicating incomplete carbonization and retention of oxygenated functional groups. Such groups enhance the adsorption capacity by improving the surface reactivity and wettability. Additionally, the absorption bands at 873 cm^{-1} and 710 cm^{-1} are associated with out-of-plane bending vibrations of aromatic C–H bonds, further confirming the dominance of aromatic structures in the biochar matrix.

3.2. Adsorption study for COD using biochar and magnetic biochar

Performance of Biochar for COD: (Abdu et al., 2025) investigated the use of TiO_2-biochar, which led to 66.6% removal of COD. The initial COD concentration was 928 mg/L, and after treatment, it was reduced to 309.9 mg/L, which is still above the discharge limit. (Pandey et al., 2023) researched immobilized on pine needle biochar for treating real textile effluents, demonstrating 33.3% COD removal. (Abdu et al., 2024) used giant reed biochar and achieved 62.7% COD removal from textile effluent.

For the present study, COD removal was evaluated across a pH range of 3–11, dosages of 0.1–2.5 g/50 mL, and contact times of 30–240 min for both PBC and PMBC. Figures 9 and 10 summarise the results.

At pH 3, both adsorbents showed the strongest performance. PBC reached 43 ± 1.1% COD removal at 0.1 g and 240 min, climbing to over 65% at dosages ≥ 1.5 g. PMBC outperformed PBC consistently: even at 0.1 g, a 47 ± 0.7% reduction was observed at 240 min, and the 2.5 g dosage achieved 88% removal. The plateau in COD removal beyond 1.5 g — visible in Figure 10(a) — indicates that available adsorption sites approach saturation at higher loadings, a well-documented behaviour in batch systems(Abdu et al., 2025).

Performance dropped substantially at neutral and alkaline pH. At pH 7, COD removal was below 25% for PMBC at any tested dose, and at pH 11, even the 2.5 g dosage achieved only 21 ± 0.6% (PMBC) and 18± 0.5% (PBC). The sharp pH dependence reflects the protonation state of surface functional groups: at pH 3, the biochar surface carries a net positive charge, thereby strengthening electrostatic attraction toward negatively charged organic species in the effluent. Hydroxyl and carboxyl groups identified in the FTIR spectrum (Section 3.1) are key contributors to this pH-mediated interaction.

Across both adsorbents, COD removal increased with contact time up to ~180 min, after which the gains were marginal. This pattern is consistent with progressive site occupation: rapid uptake in the first 60–120 min reflects adsorption onto easily accessible exterior sites. In contrast, slower uptake afterwards is governed by intraparticle diffusion into finer pores.

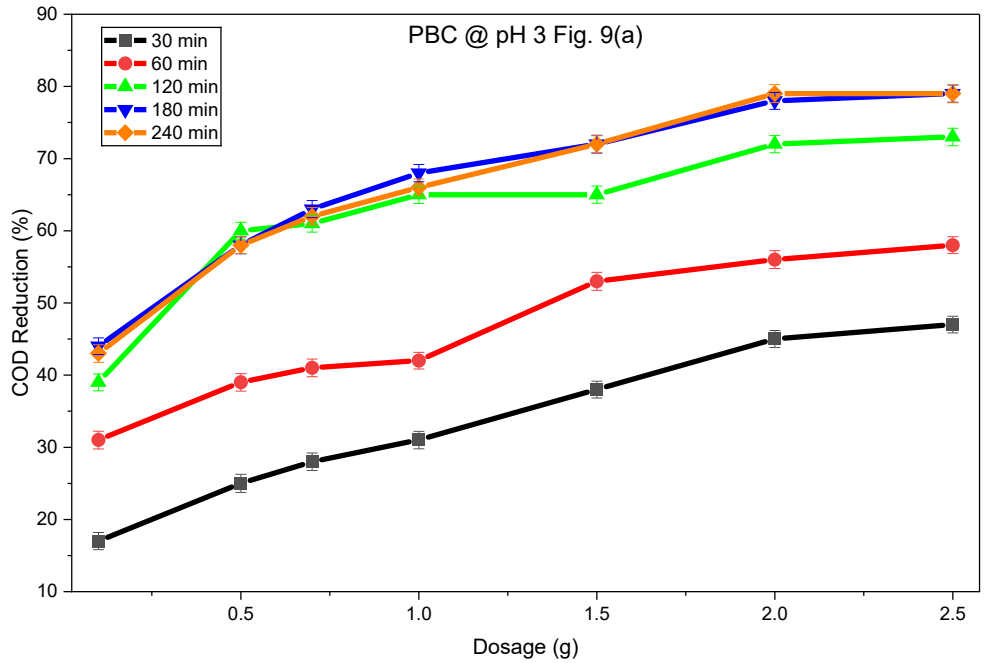
PBC @ pH 3 Fig. 9(a)
30 min
60 min
120 min
180 min
240 min
COD Reduction (%)
Dosage (g)
10
20
30
40
50
60
70
80
90
0.5
1.0
1.5
2.0
2.5

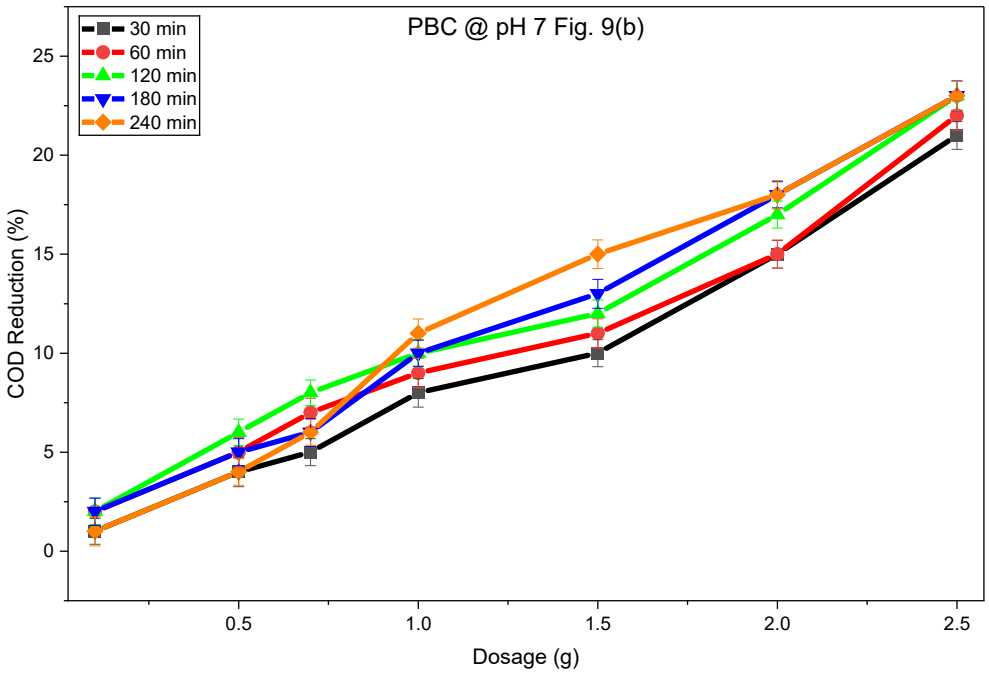
PBC @ pH 7 Fig. 9(b)
30 min
60 min
120 min
180 min
240 min
COD Reduction (%)
Dosage (g)
0
5
10
15
20
25
0.5
1.0
1.5
2.0
2.5

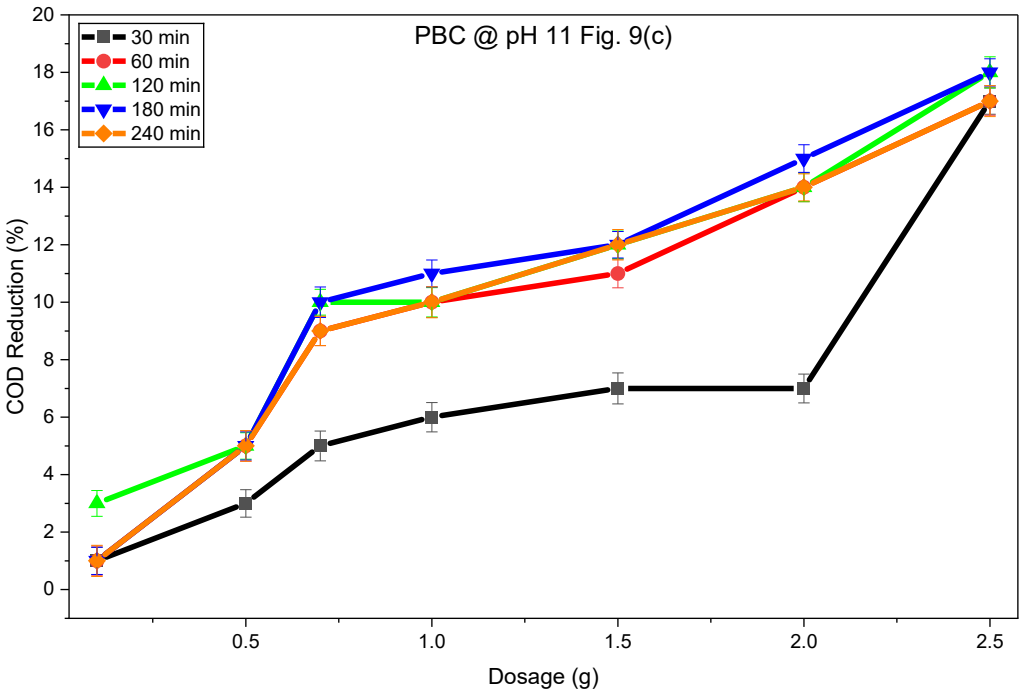

Figure 9: % COD reduction at different adsorbent dosage at varied pH using Biochar

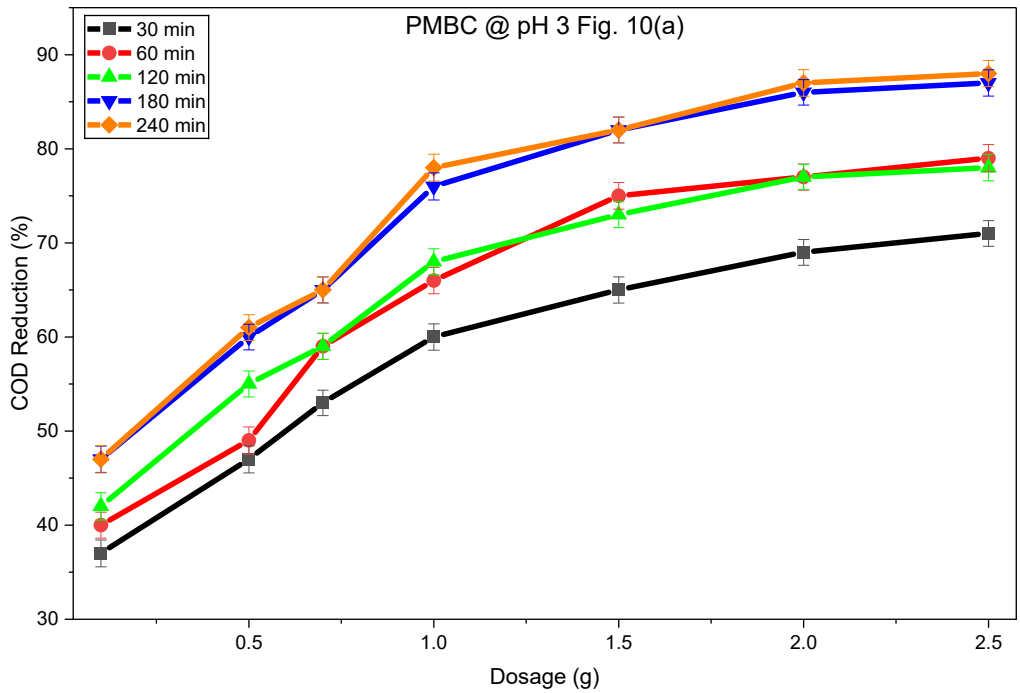

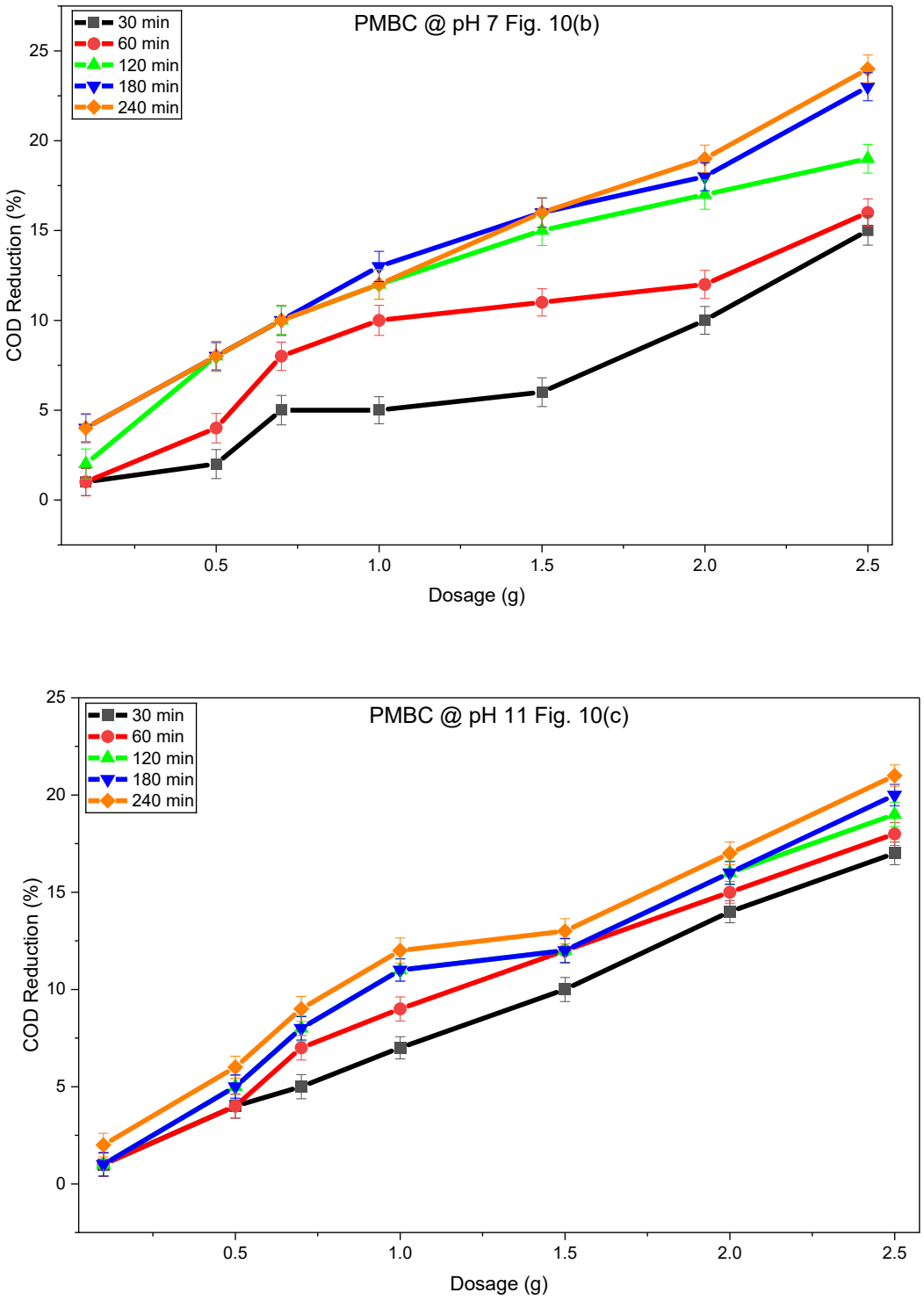

Figure 10: % COD reduction at different adsorbent dosage at varied pH using Magnetic Biochar

Although a dosage of 2.5 g/50 mL showed marginally higher COD removal (~2–3% above 2.0 g/50 mL), the incremental gain beyond 2.0 g was not statistically significant. The dosage of 2.0 g/50 mL was therefore selected as the practical optimum based on the principle of diminishing returns — higher adsorbent mass increases material cost and complicates post-treatment separation without proportionate improvement. Similarly, while COD removal at 240 min was marginally higher than at 180 min, the difference was within experimental uncertainty. A contact time of 180 min was selected as the operational optimum because it achieved near-equilibrium conditions. This approach is consistent with the cost-effective approach to selecting adsorbent doses adopted in similar studies.

A critical question is whether a high percentage removal actually translates to treated effluent meeting discharge norms. Under the optimum conditions (pH 3, 2.0 g/50 mL, 180 min), PMBC reduced COD from 1354 mg/L to 189.6 mg/L — within the permissible limit of 250 mg/L (Table 5). PBC, at 78 ± 1.2% removal, left a residual COD of 297.9 mg/L, which remains above the discharge threshold. For TDS, both adsorbents brought the concentration below the 2100 mg/L limit: PBC achieved a final TDS of 1595 mg/L, while PMBC reduced it further to 495 mg/L. These results show that PMBC can, under optimised conditions, produce COD-compliant effluent from this wastewater in a single-stage batch treatment. This finding distinguishes it from several reported adsorbents that achieve high removal percentages from lower initial concentrations. The PBC data serve as a useful reference: even at 78± 1.2% COD removal from 1354 mg/L, compliance is not reached, underscoring why magnetic modification matters for this specific effluent.

Table 5: Summary of optimum COD and TDS removal under best-performing conditions (pH 3, 2.0 g/50 mL, 180 min)

Parameter	Adsorbent	Initial (mg/L)	Final C_e (mg/L)	Removal (%)	q (mg/g)	Discharge Limit	Compliance
COD	PBC	1354	297.9	78%	26.4	250 mg/L	No
COD	PMBC	1354	189.6	86%	29.1	250 mg/L	Yes
TDS	PBC	5500	1595	71%	97.6	2100 mg/L	Yes
TDS	PMBC	5500	495	91%	125.1	2100 mg/L	Yes

3.3 Adsorption study for TDS using biochar and magnetic biochar

The same conditions were used to measure the reduction in TDS by biochar (PBC) and magnetic biochar (PMBC), with a pH range of 3-11 and a contact time of 30-240 min. **Figure 11** represents the use of biochar for TDS reduction, and **Figure 12** represents magnetic biochar for TDS reduction under the given conditions.

Performance of Biochar for TDS (Selvakumar et al., 2023) compared biochar-constructed wastelands to conventional constructed wastelands, with 53.07% and 40.04% TDS reductions, respectively (Zulti et al., 2024). Rice husk biochar was used to reduce TDS, but only to class A levels. (Chavda and Pandya, 2014) evaluated the dose of biochar and achieved a 7.3% reduction in TDS concentration at a 5g/L dosage and a 7 h contact time.

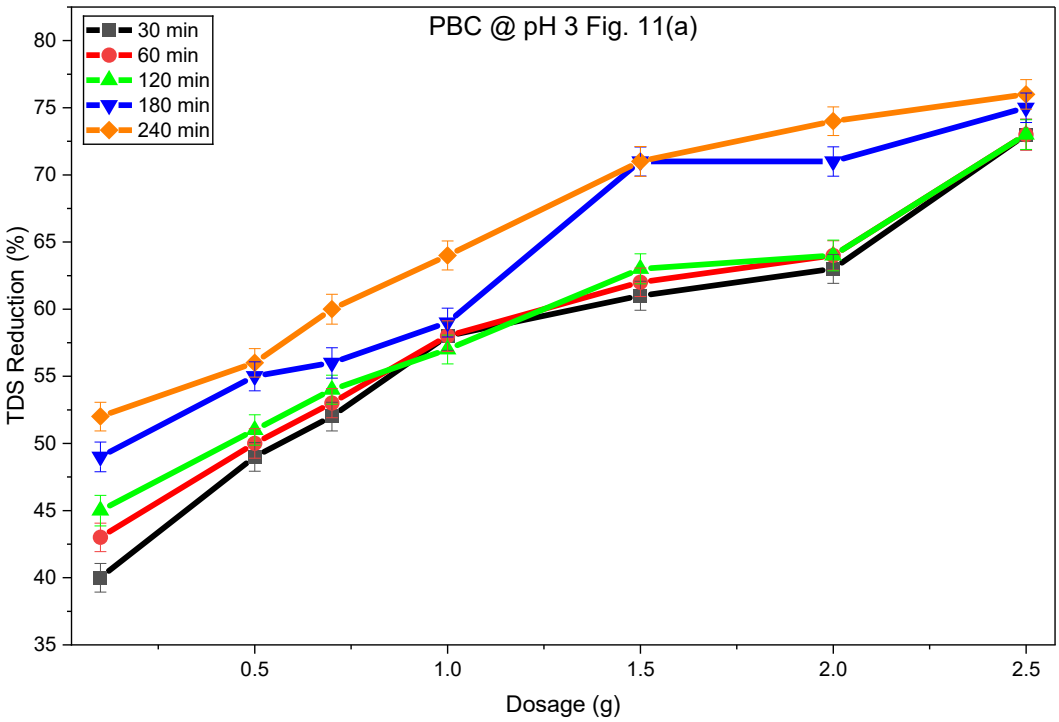
PBC @ pH 3 Fig. 11(a)
30 min
60 min
120 min
180 min
240 min
TDS Reduction (%)
Dosage (g)
35
40
45
50
55
60
65
70
75
80
0.5
1.0
1.5
2.0
2.5

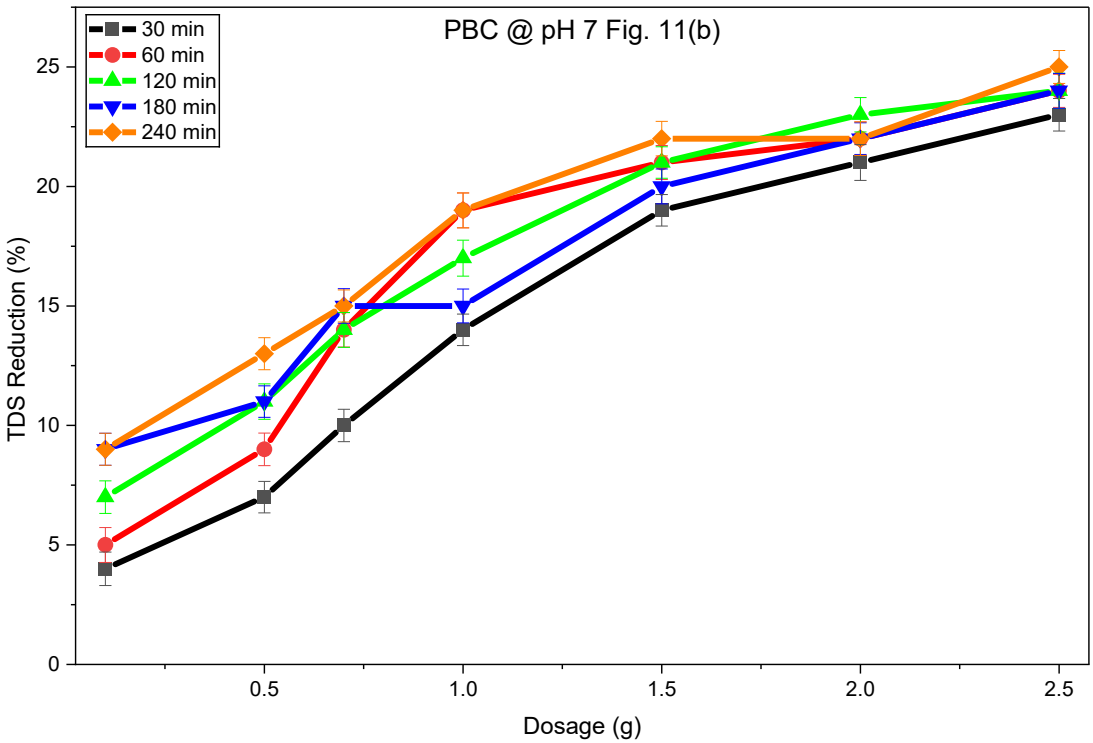
PBC @ pH 7 Fig. 11(b)
30 min
60 min
120 min
180 min
240 min
TDS Reduction (%)
Dosage (g)
0
5
10
15
20
25
0.5
1.0
1.5
2.0
2.5

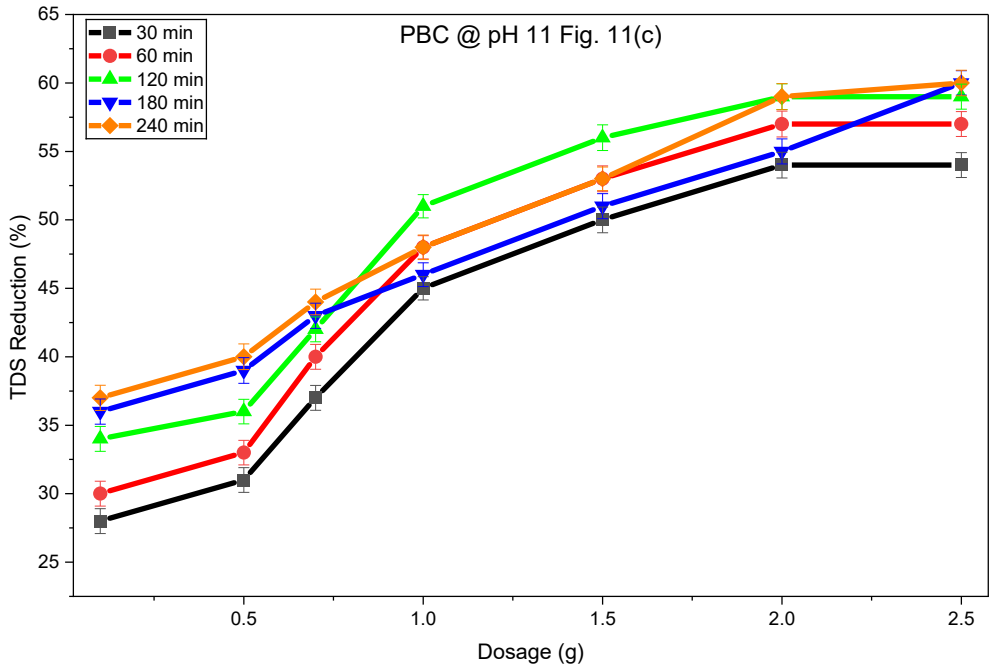

Figure 11: % TDS reduction at different adsorbent dosages at varied pH using Biochar

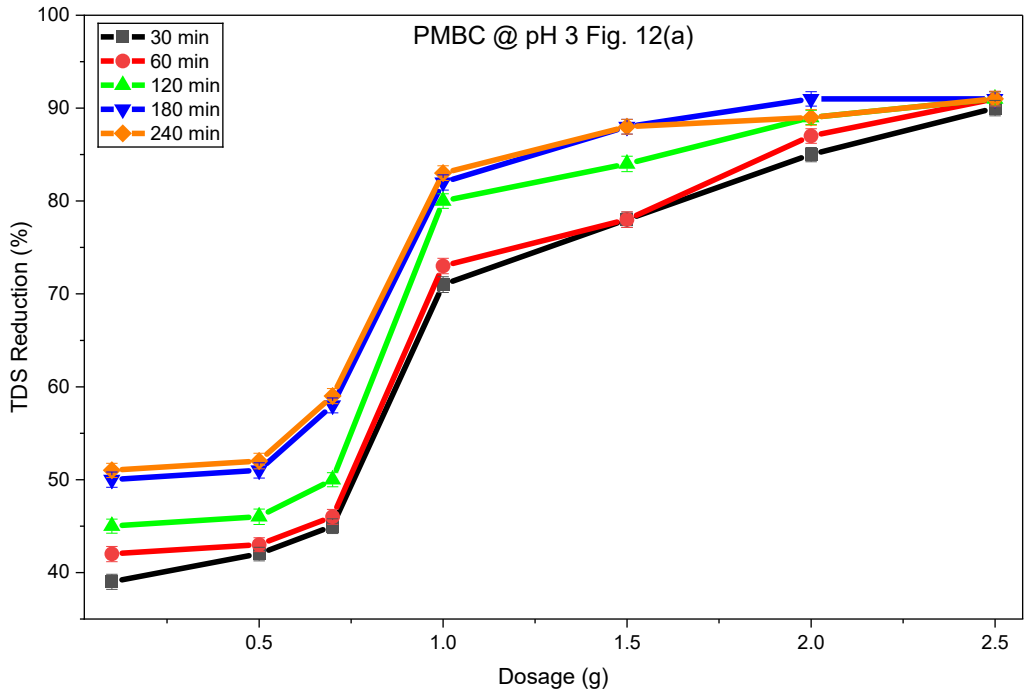

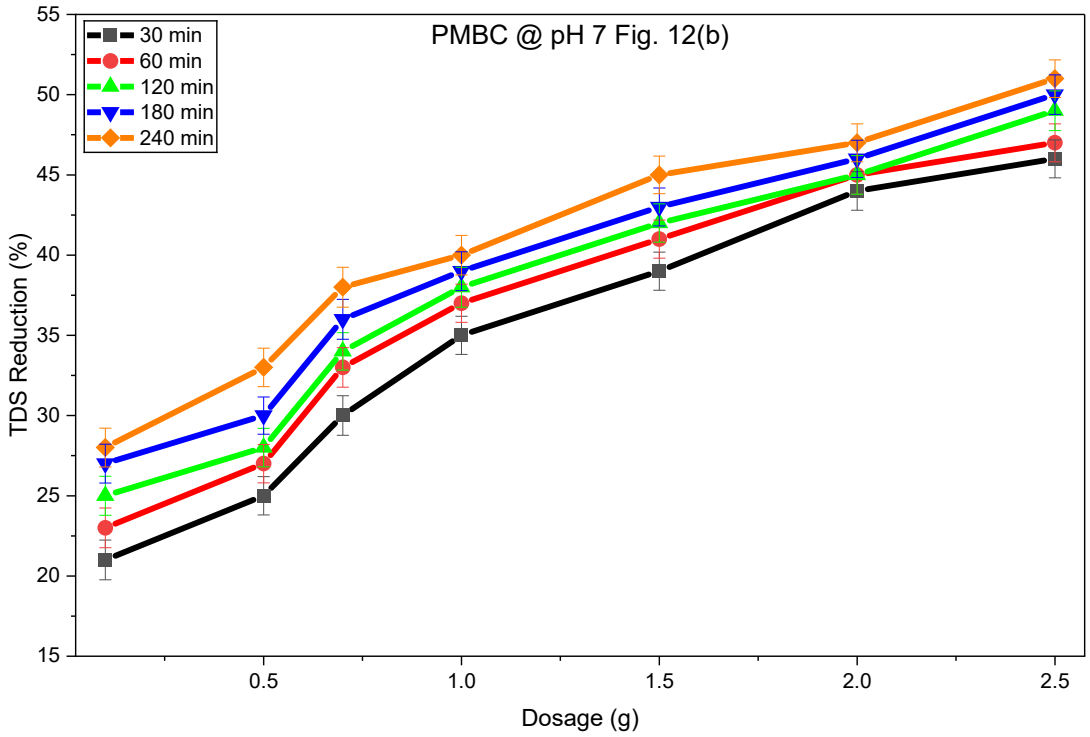

Figure 12: % TDS reduction at different adsorbent dosage at varied pH using Magnetic Biochar

TDS removal was evaluated across the same experimental conditions as COD — pH 3, 7, and 11; dosages of 0.1–2.5 g/50 mL; and contact times of 30–240 min — for both PBC and PMBC. Figures 9 and 10 summarise the results. At pH 3, both adsorbents produced their highest TDS removal. PBC removed 40 ± 1.0% at 0.1 g after 30 min, reaching 52 ± 1.3% at 240 min — a gradual 12% gain over the full contact window, suggesting the system had not

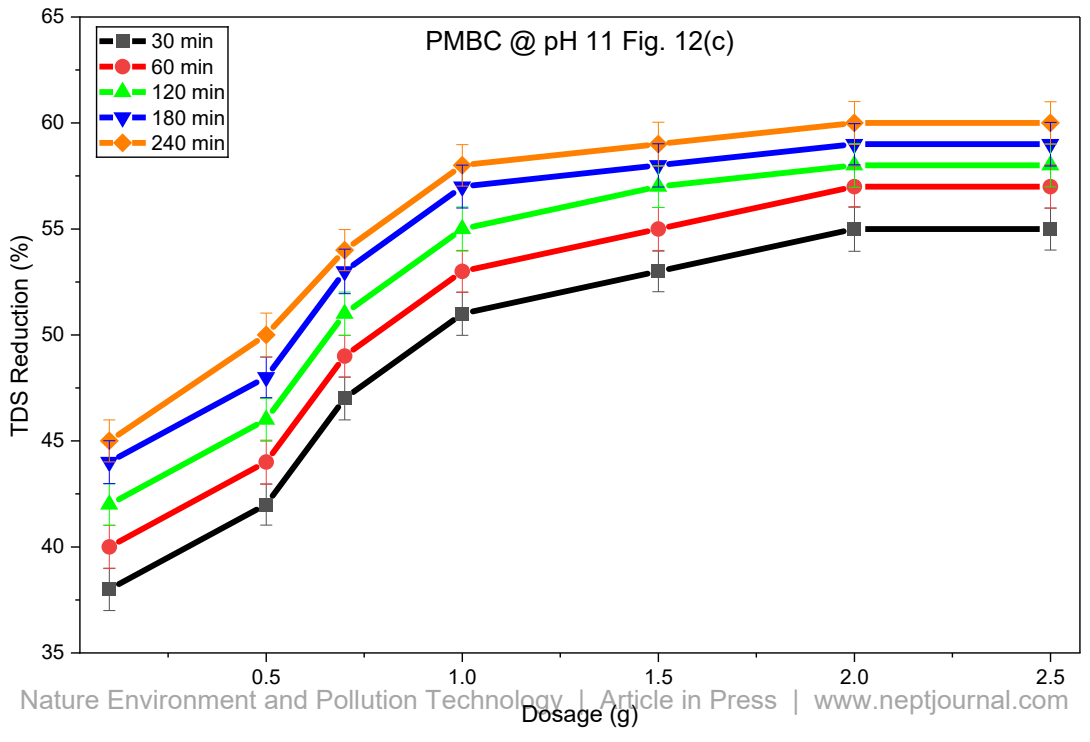

quite reached equilibrium at the lower dose. At 2.0 g and above, removal exceeded 63± 0.9% consistently, with the 2.5 g dosage reaching 76 ± 1.1% at 240 min. PMBC performed considerably better. Even at 0.1 g, a 40 ± 1.0% reduction was recorded at 30 min, rising to 52 ± 1.3% at 240 min. The step change came at higher doses: from 1.5 g onward, PMBC achieved ≥ 84% removal after 120 min, and at 2.5 g, removal was 90 ± 1.4% at 30 min and 91 ± 1.4% at 240 min — a difference of just 1 percentage point across the entire contact-time range at that loading. That near-flat plateau implies the system approached equilibrium within the first 30 min at high PMBC doses, making contact time a secondary variable under those conditions.

Performance fell sharply at neutral and alkaline pH. At pH 7, neither adsorbent exceeded 25% TDS removal regardless of dose or contact time, and the dose-response curve was unusually compressed, with very little difference between the 0.5 g and 2.5 g runs for both materials. pH 11 yielded somewhat better results, which is not immediately intuitive. PBC reached 51% removal at 2.5 g and 240 min, and PMBC achieved 59–60% under the same conditions. Gains from extending contact time were modest at pH 11 — typically 4–6% across the full-time range — suggesting equilibrium was approached quickly, even if the ceiling was far lower than at pH 3. The consistent, if moderate, improvement at pH 11 relative to pH 7 may reflect deprotonation of surface carboxyl and hydroxyl groups, which, under alkaline conditions, can interact with polar or cationic dissolved species; however, without ion-selective characterisation of the TDS fraction, this remains a proposed rather than confirmed mechanism.

Across all pH and dosage conditions, PMBC outperformed PBC for TDS removal. The gap was widest at pH 3 — 91% vs 71% at optimal conditions, a 20 percentage-point difference — and narrowed at pH 7 and 11, where neither material performed well, but PMBC held a consistent 5–10-point advantage. The iron oxide phase on PMBC likely contributes through surface complexation and electrostatic interactions with dissolved ionic species, supplementing the carbon-surface adsorption that both materials share. Separating these contributions quantitatively would require post-adsorption ion-selective or elemental analysis, which is beyond the scope of this study. The optimal removal values, equilibrium concentrations, adsorption capacities, and discharge limit compliance for both adsorbents are summarised in Table 6.

Table 6: Comparative summary of Biochar (PBC) and Magnetic Biochar (PMBC) adsorption studies

Precursor	BC/MBC	Synthesis Method	% Removal/Adsorption capacity	References
Paper mill sludge (PBC) — THIS STUDY	Biochar	Slow pyrolysis 500°C	Adsorption capacity recorded at 26.4 mg/g for COD and 97.7 mg/g for TDS removal.	This Study
Paper mill sludge (PMBC) — THIS STUDY	Magnetic Biochar	Slow pyrolysis + co-precipitation	The recorded adsorption capacities for COD and TDS removal were 29.1 mg/g and 125.1 mg/g, respectively.	This Study
Crab shell biochar	Biochar	Hydrothermal Carbonization with Acid Activation	Removed 75.33% of COD from rifapentine pharmaceutical wastewater	(Liu et al., 2025)

Physically activated cotton stalk biochar	Biochar	Pyrolysis followed by Physical and Chemical Activation	achieved 71.81% COD removal from dairy wastewater,	(Barad, 2025)
Palm Shell Magnetic Biochar	Magnetic Biochar	Pyrolysis and Co-precipitation.	Achieved 87.91% COD removal from greywater	(Andrio et al., 2024)
Bamboo biochar microspheres (Fe_3O_4@L-ABM_{500})	Magnetic Biochar	Multi-step hybrid approach combining Hydrothermal Carbonization, Chemical Activation (KOH), Organic Grafting and Co-precipitation	86.06% COD removal with a maximum adsorption capacity of 889 mg/g for oily dye wastewater	(Shen et al., 2023)

Table 6 restricts the comparison to studies targeting COD and/or TDS from dye, textile, or industrially relevant wastewater — parameters that are directly commensurable with the present study. Several observations emerge. First, most reported biochar and magnetic biochar adsorbents use agro-industrial precursors; to our knowledge, no prior study has used paper mill sludge for this specific application. Second, while magnetic biochars from palm shell and bamboo achieved comparable or slightly higher COD removal (87.9% and 86.1%, respectively), both were tested on different wastewater matrices — greywater and oily dye water — and neither reported TDS removal. Third, this study is among the few to report simultaneous COD and TDS removal from a real dye effluent with initial COD of 1354 mg/L and TDS of 5500 mg/L — concentrations considerably higher than those used in most synthetic wastewater studies. Adsorption capacity data are scarce in the literature for COD/TDS applications; the values obtained here (PMBC: 29.1 mg/g COD, 125.1 mg/g TDS) serve as a baseline for future comparative work.

4. CONCLUSION

This study demonstrated the successful valorization of paper mill sludge (PMS), an abundant industrial waste, into biochar (PBC) and magnetic biochar (PMBC) for simultaneous removal of chemical oxygen demand (COD) and total dissolved solids (TDS) from real dye wastewater. This work addresses critical gaps in the existing literature by utilizing a non-agro-industrial waste precursor and evaluating its adsorption performance using real industrial effluent rather than synthetic wastewater. Physicochemical characterization confirmed that PMS-derived biochar possesses properties favourable for adsorption, including low moisture content, appreciable fixed carbon content, and developed porosity. Proximate analysis indicated that magnetization increased the ash and fixed carbon contents, reflecting the successful incorporation of iron oxides into the biochar matrix. SEM analysis revealed that the biochar exhibited a rough, heterogeneous, and porous surface with numerous voids and crevices, facilitating

mass transfer and physisorption. The BET analysis confirmed that activated PMBC exhibited a surface area exceeding 600 m^2/g, consistent with a highly microporous structure, while PBC showed a surface area of 48.2 m^2/g, aligning with previously reported values for paper mill sludge biochar. The magnetic biochar showed partial surface coverage by iron-based particles, indicating successful magnetization while preserving the surface roughness. The FTIR spectra confirmed the presence of oxygen-containing functional groups (hydroxyl, carbonyl, carboxyl, and ether groups) and aromatic structures, suggesting that adsorption occurred through a combination of hydrogen bonding, electrostatic interactions, surface complexation, and π–π interactions. Batch adsorption experiments showed that the solution pH, adsorbent dosage, and contact time significantly influenced COD and TDS removal. Acidic conditions (pH 3) consistently yielded the highest removal efficiencies, owing to enhanced surface protonation and favourable electrostatic interactions. Increasing the adsorbent dosage improved the removal efficiency by increasing the number of available adsorption sites, although a plateau was observed at higher dosages, indicating saturation. Adsorption equilibrium is generally achieved within 120–240 min, beyond which only marginal improvements are observed. Under optimised conditions, PMBC reduced COD from 1354 mg/L to 189.6 mg/L, achieving compliance with the permissible discharge limit of 250 mg/L, while PBC left a residual COD of 297.9 mg/L, which remained above the threshold. For TDS, both adsorbents achieved compliance: PBC reduced TDS to 1595 mg/L and PMBC to 495 mg/L, against the permissible limit of 2100 mg/L.

The magnetic biochar consistently outperformed the nonmagnetic biochar across all tested conditions. Under optimized operating conditions (pH 3, adsorbent dosage of 2.0 g per 50 mL, and contact time of 180 minutes), biochar achieved COD and TDS removal efficiencies of 78±1.2% and 71±1.1%, respectively. In contrast, magnetic biochar achieved significantly higher COD and TDS removal efficiencies of 86±1.4% and 91±1.2%, respectively. The enhanced performance of magnetic biochar is attributed to the improved surface characteristics, increased availability of active adsorption sites, and synergistic interactions introduced by iron oxides. Additionally, magnetic biochar offers the practical advantage of easy separation from treated effluent using an external magnetic field. In comparison with reported studies, the performance of PMS-derived biochar and magnetic biochar is competitive or superior, particularly when considering the use of real dye wastewater and simultaneous COD and TDS removal. Overall, this study establishes paper mill sludge as a viable precursor for producing effective and sustainable adsorbents and highlights magnetic biochar as a promising material for industrial wastewater treatment and circular economy applications.

Author Contributions

- Charmiben Panchani: Conceptualization, Methodology, Formal analysis, Writing – original draft.
- Vishwa Vraj Shah: Supervision, Project administration, Validation, Data curation.
- Ahaan Thakore: Investigation, Writing – original draft, writing – review, and editing.

Acknowledgments: The authors wish to express their gratitude to the dye manufacturing facility in Gujarat and the paper mill in Ankleshwar, Gujarat, India for providing the effluent and sludge samples necessary for this research.

Declaration of Generative AI and AI-Assisted Technologies in the Writing Process: The authors used ChatGPT (GPT- 4o) and AI visualization tools only for infographic and graphical abstract design. These tools were not involved in manuscript drafting, data interpretation, or conclusions. Authors reviewed all outputs and assume full responsibility for final content.

Funding Statement: The authors received no specific funding for this work.

Conflicts of Interest Disclosure: The authors declare that they have no known competing financial interests or personal relationships that influenced the work reported in this paper.

Data Availability Statement: The data that support the findings of this study are available from the corresponding author upon reasonable request.

REFERENCES

A G, M., R K, K., M, B., T, U., M, S., T, R., D, M., 2026. Sustainable management of paper mill sludge: insights from advanced instrumental characterization. Int. J. Environ. Anal. Chem. 106, 896–924. https://doi.org/10.1080/03067319.2025.2527775

Abdu, M., Babaee, S., Worku, A., Diale, P., Msagati, T.A.M., Nure, J.F., 2025. Synthesis and optimization of TiO2-biochar composite for degradation of Basic Blue 41 dye in textile wastewater using response surface methodology. Inorg. Chem. Commun. 174, 114078. https://doi.org/10.1016/j.inoche.2025.114078

Abdu, M., Babaee, S., Worku, A., Msagati, T.A.M., Nure, J.F., 2024. The development of Giant reed biochar for adsorption of Basic Blue 41 and Eriochrome Black T. azo dyes from wastewater. Sci. Rep. 14, 18320. https://doi.org/10.1038/s41598-024-67997-5

Al-Tameemi, H., Jabbar, M., Bader, A., 2022. BOD: COD Ratio as Indicator for Wastewater and Industrial Water Pollution.

Al-Tohamy, R., Ali, S.S., Li, F., Okasha, K.M., Mahmoud, Y.A.-G., Elsamahy, T., Jiao, H., Fu, Y., Sun, J., 2022. A critical review on the treatment of dye-containing wastewater: Ecotoxicological and health concerns of textile dyes and possible remediation approaches for environmental safety. Ecotoxicol. Environ. Saf. 231, 113160. https://doi.org/10.1016/j.ecoenv.2021.113160

Amini, E., Safdari, M.-S., DeYoung, J.T., Weise, D.R., Fletcher, T.H., 2019. Characterization of pyrolysis products from slow pyrolysis of live and dead vegetation native to the southern United States. Fuel 235, 1475–1491. https://doi.org/10.1016/j.fuel.2018.08.112

Andrio, D., Saputra, M.R., Darmayanti, L., 2024. Utilization of Magnetic Biochar from Palm Shell as An Adsorbent for Removal of COD, Total Suspended Solid, Oil and Grease in Greywater. J. Penelit. Pendidik. IPA 10, 1195–1204. https://doi.org/10.29303/jppipa.v10i3.4597

Barad, A.K., 2025. ACTIVATED BIO CHAR: A HIGHLY EFFECTIVE ADSORBENT FOR THE REMOVAL OF CONTAMINANTS FROM DAIRY WASTEWATER. Plant Arch. 25. https://doi.org/10.51470/PLANTARCHIVES.2025.v25.SP.ICTPAIRS-068

Chavda, S.B., Pandya, M.J., 2014. Evaluation of Removal of TDS, COD and Heavy metals from Wastewater using Biochar 1.

Chistie, S.M., Naik, S.U., Rajendra, P., Apeksha, Mishra, R.K., Albasher, G., Chinnam, S., Jeppu, G.P., Arif, Z., Hameed, J., 2025. Production and characterization of magnetic Biochar derived from pyrolysis of waste areca nut husk for removal of methylene blue dye from wastewater. Sci. Rep. 15, 23209. https://doi.org/10.1038/s41598-025-03359-z

Devi, P., Saroha, A.K., 2014a. Optimization of Pyrolysis Conditions to Synthesize Adsorbent from Paper Mill Sludge. J. Clean Energy Technol. 180–182. https://doi.org/10.7763/JOCET.2014.V2.118

Devi, P., Saroha, A.K., 2014b. Synthesis of the magnetic biochar composites for use as an adsorbent for the removal of pentachlorophenol from the effluent. Bioresour. Technol. 169, 525–531. https://doi.org/10.1016/j.biortech.2014.07.062

Devi, P., Saroha, A.K., n.d. Effect Of Temperature On Biochar Properties During Paper Mill Sludge Pyrolysis.

Dhinesh, R., Aruna, S., Manikandavelu, D., Ravaneswaran, K., Kirthiga, S.S., Al-Ghanim, K.A., Kamaraj, C., 2024. Naturally derived organic biochar as an alternative to commercially activated carbon in the oxygen removal of seafood processing wastewater. J. Chem. Technol. Biotechnol. 99, 1691–1702. https://doi.org/10.1002/jctb.7664

Fakhar, A., Galgo, S.J.C., Canatoy, R.C., Rafique, M., Sarfraz, R., Farooque, A.A., Khan, M.I., 2025. Advancing modified biochar for sustainable agriculture: a comprehensive review on characterization, analysis, and soil performance. Biochar 7, 8. https://doi.org/10.1007/s42773-024-00397-0

Guel-Nájar, N.A., Rios-Hurtado, J.C., Muzquiz-Ramos, E.M., Dávila-Pulido, G.I., González-Ibarra, A.A., Pat-Espadas, A.M., 2023. Magnetic Biochar Obtained by Chemical Coprecipitation and Pyrolysis of Corn Cob Residues: Characterization and Methylene Blue Adsorption. Materials 16, 3127. https://doi.org/10.3390/ma16083127

Habila, M.A., Moshab, M.S., El-Toni, A.M., ALOthman, Z.A., Badjah Hadj Ahmed, A.Y., 2023. Thermal Fabrication of Magnetic Fe3O4 (Nanoparticle)@Carbon Sheets from Waste Resources for the Adsorption of Dyes: Kinetic, Equilibrium, and UV–Visible Spectroscopy Investigations. Nanomaterials 13, 1266. https://doi.org/10.3390/nano13071266

Husien, S., El-taweel, R.M., Salim, A.I., Fahim, I.S., Said, L.A., Radwan, A.G., 2022. Review of activated carbon adsorbent material for textile dyes removal: Preparation, and modelling. Curr. Res. Green Sustain. Chem. 5, 100325. https://doi.org/10.1016/j.crgsc.2022.100325

Igalavithana, A.D., Choi, S.W., Shang, J., Hanif, A., Dissanayake, P.D., Tsang, D.C.W., Kwon, J.-H., Lee, K.B., Ok, Y.S., 2020. Carbon dioxide capture in biochar produced from pine sawdust and paper mill sludge: Effect of porous structure and surface chemistry. Sci. Total Environ. 739, 139845. https://doi.org/10.1016/j.scitotenv.2020.139845

Ishar, ., Paulina, T., . F., 2024. Effectiveness of Activated Carbon from Nutmeg Shell (Myristica fragrans) Waste as Adsorbent for Metal Ions Pb(II) and Cu(II) in Liquid Waste. Nat. Environ. Pollut. Technol. 23, 1075–1083. https://doi.org/10.46488/NEPT.2024.v23i02.041

Islam, Md.M., Aidid, A.R., Mohshin, J.N., Mondal, H., Ganguli, S., Chakraborty, A.K., 2025. A critical review on textile dye-containing wastewater: Ecotoxicity, health risks, and remediation strategies for environmental safety. Clean. Chem. Eng. 11, 100165. https://doi.org/10.1016/j.clce.2025.100165

Kan, T., Strezov, V., Evans, T.J., 2016. Lignocellulosic biomass pyrolysis: A review of product properties and effects of pyrolysis parameters. Renew. Sustain. Energy Rev. 57, 1126–1140. https://doi.org/10.1016/j.rser.2015.12.185

Kathing, C., Saini, G., 2022. A Review of Various Treatment Methods for the Removal of Dyes from Textile Effluent. Recent Prog. Mater. 4, 1–15. https://doi.org/10.21926/rpm.2204028

Leng, L., Huang, H., Li, H., Li, J., Zhou, W., 2019. Biochar stability assessment methods: A review. Sci. Total Environ. 647, 210–222. https://doi.org/10.1016/j.scitotenv.2018.07.402

Liang, M., Ding, Y., Zhang, Q., Wang, D., Li, H., Lu, L., 2020. Removal of aqueous Cr(VI) by magnetic biochar derived from bagasse. Sci. Rep. 10, 21473. https://doi.org/10.1038/s41598-020-78142-3

Lima, D.R., Hosseini-Bandegharaei, A., Thue, P.S., Lima, E.C., de Albuquerque, Y.R.T., dos Reis, G.S., Umpierres, C.S., Dias, S.L.P., Tran, H.N., 2019. Efficient acetaminophen removal from water and hospital effluents treatment by activated carbons derived from Brazil nutshells. Colloids Surf. Physicochem. Eng. Asp. 583, 123966. https://doi.org/10.1016/j.colsurfa.2019.123966

Liu, J., Wen, Q., Xu, M., Wu, Y., Guo, X., 2025. Investigating the adsorption performance of calcium-rich biochar on CDOM from actual rifapentine pharmaceutical wastewater using spectroscopic techniques. Environ. Sci. Water Res. Technol. 11, 914–924. https://doi.org/10.1039/D4EW01002G

Lv, Q., Wang, H., Zhang, M., Xue, J., Yang, J., 2020. Synthesis of magnetic biochar/carbonate intercalated Mg–Al layered double hydroxides for enhanced Cd(II) removal from aqueous solution. Desalination Water Treat. 207, 258–269. https://doi.org/10.5004/dwt.2020.26428

Muzenda, C., Arotiba, O.A., 2022. Improved Magnetite Nanoparticle Immobilization on a Carbon Felt Cathode in the Heterogeneous Electro-Fenton Degradation of Aspirin in Wastewater. ACS Omega 7, 19261–19269. https://doi.org/10.1021/acsomega.2c00627

Niu, J., Fan, S., Wu, Z., 2025. Preparation of Biochar from Papermaking Sludge and Its Adsorption Characteristics for Tetracycline. Toxics 13, 1050. https://doi.org/10.3390/toxics13121050

Nizam, N.U.M., Hanafiah, M.M., Mahmoudi, E., Halim, A.A., Mohammad, A.W., 2021. The removal of anionic and cationic dyes from an aqueous solution using biomass-based activated carbon. Sci. Rep. 11, 8623. https://doi.org/10.1038/s41598-021-88084-z

Oliveira, L.C.A., Rios, Rachel.V.R.A., Fabris, J.D., Garg, V., Sapag, K., Lago, R.M., 2002. Activated carbon/iron oxide magnetic composites for the adsorption of contaminants in water. Carbon 40, 2177–2183. https://doi.org/10.1016/S0008-6223(02)00076-3

Pandey, D., Daverey, A., Dutta, K., Arunachalam, K., 2023. Dye removal from simulated and real textile effluent using laccase immobilized on pine needle biochar. J. Water Process Eng. 53, 103710. https://doi.org/10.1016/j.jwpe.2023.103710

Santhosh, C., Daneshvar, E., Tripathi, K.M., Baltrėnas, P., Kim, T., Baltrėnaitė, E., Bhatnagar, A., 2020. Synthesis and characterization of magnetic biochar adsorbents for the removal of Cr(VI) and Acid orange 7 dye from aqueous solution. Environ. Sci. Pollut. Res. Int. 27, 32874–32887. https://doi.org/10.1007/s11356-020-09275-1

Sayğılı, H., Güzel, F., 2016. Effective removal of tetracycline from aqueous solution using activated carbon prepared from tomato (*Lycopersicon esculentum* Mill.) industrial processing waste. Ecotoxicol. Environ. Saf. 131, 22–29. https://doi.org/10.1016/j.ecoenv.2016.05.001

Selvakumar, S., Boomiraj, K., Durairaj, S., Veluswamy, K., 2023. Performance evaluation of a lab-scale subsurface flow-constructed wetland system for textile industry wastewater treatment. Environ. Sci. Pollut. Res. Int. 30, 102708–102724. https://doi.org/10.1007/s11356-023-29425-5

Shen, L., Jin, R., Chen, W., Qi, D., Zhai, S., 2023. Preparation of Biochar Composite Microspheres and Their Ability for Removal with Oil Agents in Dyed Wastewater. Materials 16, 6155. https://doi.org/10.3390/ma16186155

Simões dos Reis, G., Bergna, D., Tuomikoski, S., Grimm, A., Lima, E.C., Thyrel, M., Skoglund, N., Lassi, U., Larsson, S.H., 2022. Preparation and Characterization of Pulp and Paper Mill Sludge-Activated Biochars Using Alkaline Activation: A Box–Behnken Design Approach. ACS Omega 7, 32620–32630. https://doi.org/10.1021/acsomega.2c04290

Tanveer, R., Yasar, A., Nizami, A.-S., Tabinda, A.B., 2023. Integration of physical and advanced oxidation processes for treatment and reuse of textile dye-bath effluents with minimum area footprint. J. Clean. Prod. 383, 135366. https://doi.org/10.1016/j.jclepro.2022.135366

Turner, T., Wheeler, R., Oliver, I.W., 2022. Evaluating land application of pulp and paper mill sludge: A review. J. Environ. Manage. 317, 115439. https://doi.org/10.1016/j.jenvman.2022.115439

Wang, X., Jiang, J., Gao, W., 2022. Reviewing textile wastewater produced by industries: characteristics, environmental impacts, and treatment strategies. Water Sci. Technol. 85, 2076–2096. https://doi.org/10.2166/wst.2022.088

Weber, K., Quicker, P., 2018. Properties of biochar. Fuel 217, 240–261. https://doi.org/10.1016/j.fuel.2017.12.054

Zhang, Z., Wang, T., Zhang, H., Liu, Y., Xing, B., 2021. Adsorption of Pb(II) and Cd(II) by magnetic activated carbon and its mechanism. Sci. Total Environ. 757, 143910. https://doi.org/10.1016/j.scitotenv.2020.143910

Zhao, Q., Xu, T., Song, X., Nie, S., Choi, S.-E., Si, C., 2021. Preparation and Application in Water Treatment of Magnetic Biochar. Front. Bioeng. Biotechnol. 9. https://doi.org/10.3389/fbioe.2021.769667

Zulti, F., Setiadewi, N., Waluyo, A., Susanti, E., 2024. Removal Pollutants in Textile Wastewater Using Unmodified Rice Husk. E3S Web Conf. 483, 02008. https://doi.org/10.1051/e3sconf/202448302008